LA-3585-MS

C.3

CIC-14 REPORT COLLECTION
REPRODUCTION
COPY

LOS ALAMOS SCIENTIFIC LABORATORY
of the
University of California
LOS ALAMOS • NEW MEXICO

Heat Pipe Capability Experiments

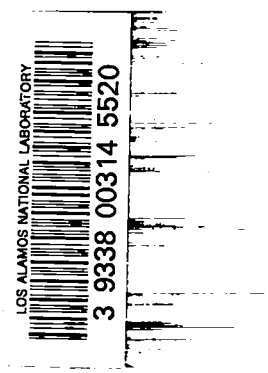

UNITED STATES
ATOMIC ENERGY COMMISSION
CONTRACT W-7405-ENG. 36

LEGAL NOTICE

This report was prepared as an account of Government sponsored work. Neither the United States, nor the Commission, nor any person acting on behalf of the Commission:

A. Makes any warranty or representation, expressed or implied, with respect to the accuracy, completeness, or usefulness of the information contained in this report, or that the use of any information, apparatus, method, or process disclosed in this report may not infringe privately owned rights; or

B. Assumes any liabilities with respect to the use of, or for damages resulting from the use of any information, apparatus, method, or process disclosed in this report.

As used in the above, "person acting on behalf of the Commission" includes any employee or contractor of the Commission, or employee of such contractor, to the extent that such employee or contractor of the Commission, or employee of such contractor prepares, disseminates, or provides access to, any information pursuant to his employment or contract with the Commission, or his employment with such contractor.

All LA...MS reports are informal documents, usually prepared for a special purpose and primarily prepared for use within the Laboratory rather than for general distribution. This report has not been edited, reviewed, or verified for accuracy. All LA...MS reports express the views of the authors as of the time they were written and do not necessarily reflect the opinions of the Los Alamos Scientific Laboratory or the final opinion of the authors on the subject.

Printed in USA. Price $ 2.00. Available from the Clearinghouse for Federal Scientific and Technical Information, National Bureau of Standards, United States Department of Commerce, Springfield, Virginia

LA-3585-MS
UC-34, PHYSICS
TID-4500

LOS ALAMOS SCIENTIFIC LABORATORY
of the
University of California
LOS ALAMOS • NEW MEXICO

Report written: August 22, 1966
Report distributed: October 27, 1966

Heat Pipe Capability Experiments

by

J. E. Kemme

ABSTRACT

Axial heat transfer limits were determined for several heat pipe systems having the same outside dimensions, but different wick configurations. Measurements were made at temperatures from 450 to 850°C by using potassium and sodium as working fluids. The wicks consisted of many axial channels, evenly spaced around the inside circumference of each container tube. Different size channels were studied; and, in some tests, a layer of fine screen was used to cover the channels and separate them from the vapor passage. The experiments were chosen to show some possible methods for wick improvement and to check the validity of existing heat pipe equations.

At higher test temperatures, good agreement was obtained between measured and calculated heat transfer limits. At low temperatures, however, heat transfer capability was below that predicted by theory, and startup difficulties were encountered with the open channel systems. These problems appear due to an interaction between low density, high velocity vapor and returning liquid. The screen covering helped startup and substantially increased heat transfer capability at all operating temperatures.

Acknowledgement

This investigation was aided considerably by the technical assistance of E. S. Keddy and A. G. Vaughan.

Introduction

A heat pipe system which has received considerable attention consists of a sealed tube lined internally with a capillary network called a wick. Application of heat to a portion of the tube causes evaporation of working fluid with which the wick is saturated. Heat is transferred through a central passage to the remainder of the system as latent energy by flow and condensation of vapor. To complete the flow cycle, the condensate is returned through the wick to the heated section by capillary forces.

Equations have been developed for estimating the axial heat transfer capability of cylindrical heat pipes as a function of temperature for different heat pipe sizes, various working fluids and certain wick configurations. Since heat pipe size and choice of working fluid will generally be determined by usage, the suitability of a heat pipe for a specific application will depend to a large extent on wick configuration.

The experiments described in this report were chosen to show some possible methods for wick improvement and to check the validity of existing heat pipe equations. To accomplish this purpose, axial heat transfer limits were determined for several heat pipe systems having the same outside dimensions, but different wick configurations. Measurements were made at temperatures from 450 to 850°C by using potassium and sodium as working fluids. During these experiments, particular attention was devoted to startup and low temperature operation since these transient conditions are difficult to treat theoretically.

Heat Transfer Limitations

Heat pipes are normally operated by adding heat radially through a section of the container wall and saturated wick. When a large enough area is used for heat addition, vapor is formed primarily by evaporation from the inside surface of the wick. As long as this condition is maintained, the input heat rate can be increased until the drag of vapor and liquid within the system equals the maximum capillary force which can be provided by the wick structure. If more heat is added, insufficient

liquid will be returned to the evaporator and normal heat pipe operation will cease. This limitation determines maximum heat transfer in an axial direction and is of interest in all heat pipe applications.

Although this report concerns only axial heat pipe limitations, it should be noted that heat transfer can also be limited by radial heat flow if the input heat flux is sufficient to produce sizeable vapor bubbles in the saturated wick. Such localized boiling can cause serious overheating in the evaporator region and interfere with the return of liquid. This limitation will exist if too small an area is required for heat addition. However, boiling may not be a problem in many heat pipe applications where liquid metal fluids and thin wicks are used to conduct heat radially. High input heat fluxes (100 to 400 W/cm^2) have been achieved in such systems, depending on the fluid used and the wick configuration.

Wick Importance

Wick construction is particularly important in heat pipe design because this structure is the capillary pump for fluid circulation and the path for liquid return. A saturated wick is also the conductor for heat flow into the system and can limit radial as well as axial heat transfer. Many types of wicks have been suggested for heat pipe use, but no single structure appears ideally suited for all applications. Two-component wicks are featured in this investigation because they provide a means for increasing heat pipe performance by utilizing fine pores for fluid pumping and a less restrictive flow path for liquid return.

Heat Pipe Construction

Experimental heat pipes were constructed from flat nickel sheets rolled into cylindrical tubes about 3/4-inch O.D. x 12-inches long. Prior to rolling, a capillary network was formed by cutting many rectangular channels along the complete length of each sheet. The width and depth of these channels were varied for different sheets. After rolling,

the tubes were seam-welded, rounded and straightened to obtain uniform outside dimensions. Short sections were then removed from the ends of each tube so that internal dimensions could be accurately measured. Some heat pipe cross sections showing arrangement and shape of channels are presented in Fig. 1.

Heat pipe construction was completed by welding nickel caps into the ends of the tubes. One of the caps contained a 1/8-inch-O.D. thermocouple well to allow temperature measurements along the length of the vapor passage. A 1/4-inch-O.D. nickel tube was located in the other cap to permit addition of working fluid.

After each heat pipe was tested with open capillary channels, a layer of fine-mesh screen was added to cover the channels and separate them from the vapor passage. The screen was pressed against the inside heat pipe wall by drawing a tapered mandrel through the assembly. The systems were then tested to determine the effect of a tight screen covering. Later, some heat pipes were tested with loose fitting screen to show the effect of screen fit.

Final Heat Pipe Preparation

Pure fluids are required for proper heat pipe operation. Otherwise, those impurities more volatile than the fluid will be driven to the condenser end of the heat pipe, creating a cold zone during operation. Container stresses and mass transport can occur because of such localized temperature gradients. Less volatile impurities will collect in the evaporator and may clog or corrode the wick, causing hot spots and reducing heat transfer. All the experimental heat pipes were filled by direct vacuum distillation to reduce impurities in the working fluid.

The filling procedure can best be described by referring to a sketch of the distillation system and attached heat pipe shown in Fig. 2. This entire system was first vacuum-outgassed for 4 hours at 900°C. Enough fluid was then added to the distillation pot to fill the voids in the heat pipe capillary structure. Heaters and thermocouples were

Fig. 1. Heat Pipe Cross Sections Showing Arrangement and Shape of Channels

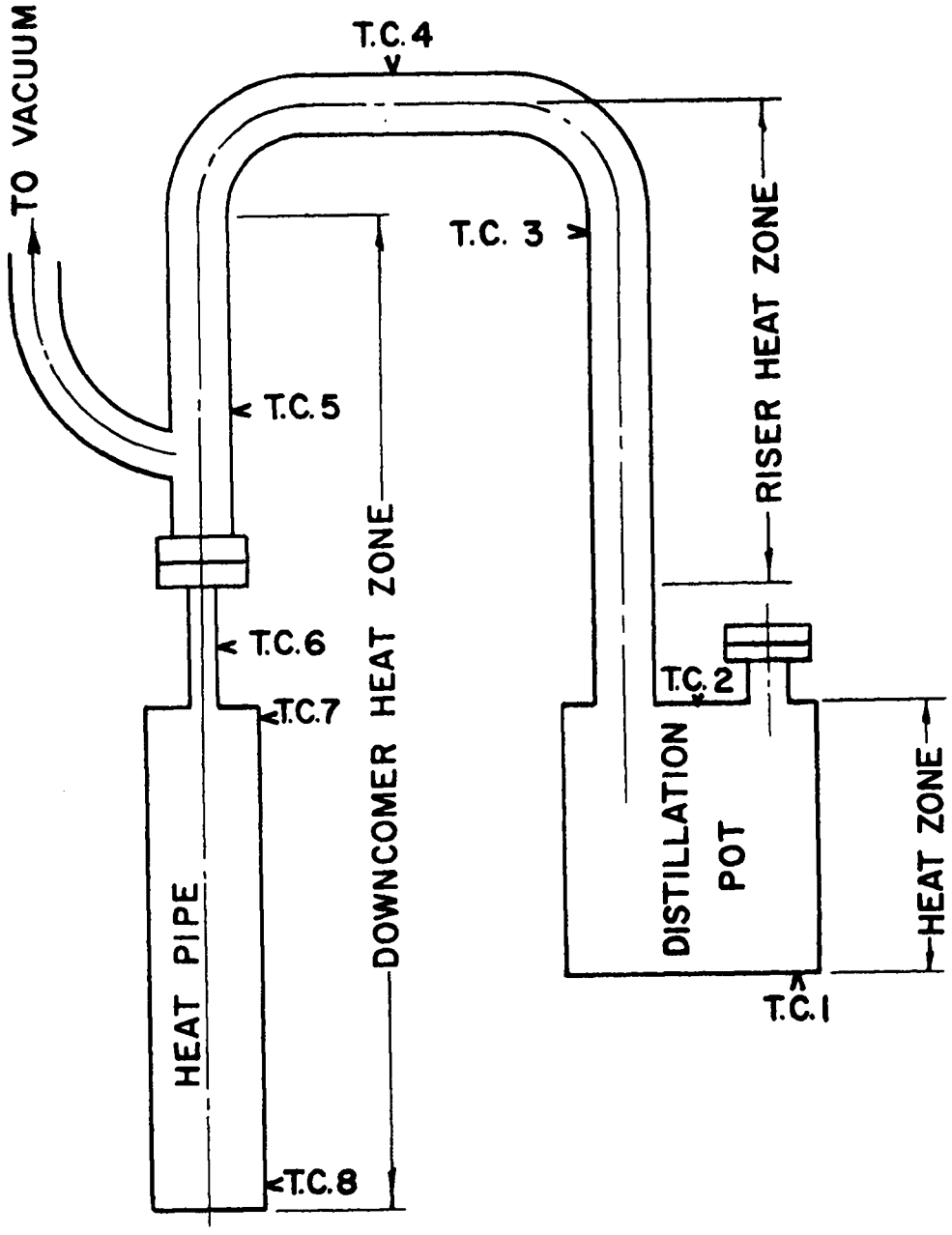

Fig. 2. Direct Distillation System

provided to permit separate temperature control of three zones: the distillation pot, the refluxing riser leg and the liquid downcomer and heat pipe. For potassium additions, the downcomer and heat pipe were first heated to 100°C, the riser was then heated to 350°C and finally the distillation pot was heated to 400°C. For sodium additions, the temperature of the downcomer and heat pipe was increased to 150°C, and the riser and distillation pot were brought to 450°C and 500°C, respectively. When refluxing and distillation began, the riser and then the downcomer showed a significant temperature increase. The distillation pot rose in temperature when distillation was complete. During fluid transfer, continuous tapping of the downcomer leg was required to prevent accumulation of liquid in this portion of the system.

After filling, the 1/4-inch nickel tube was flattened and pinched off near the heat pipe. This pinch-off was then welded in an inert gas atmosphere or in an electron-beam vacuum chamber. Prior to testing, the completed heat pipes were furnace heated at 800°C for 60 hours to allow the fluid to wet the capillary structure.

Experimental Procedure

An accommodating heat removal system must be provided to assure startup of heat pipes with liquid metal fluids. Heat transfer rates should be kept small, especially prior to melting of the liquid metal and at very low fluid vapor pressures. This is an important aspect of heat pipe operation and will be discussed in greater detail later in this report.

The experimental procedure used in this investigation involved heat removal by conduction through a narrow gas annulus to a water calorimeter. Heat transfer rates were kept low during startup by using argon in the gas annulus until a desired heat pipe temperature was reached. Heat transfer was then varied at this temperature by using different mixtures of argon and helium in the gas annulus. Heat removal rates were continuously measured during operation by monitoring the temperature

rise and circulation rate of water through the calorimeter. Since the temperature of the water never exceeded 50°C, the calorimeter measurements provided a direct and convenient method for determining axial heat transfer in all of the experiments.

A sketch of the heat transfer apparatus is shown in Fig. 3. The calorimeter consisted of two copper tubes arranged to form an annular passage for circulating water. During a test, the condenser section of a heat pipe was located within this cooling jacket with spacers to provide a gas annulus. The length of the condenser section was 22 cm, and the width of the gas annulus was 25 mils at room temperature. Input power was supplied by an induction coil surrounding that portion of the heat pipe outside of the cooling jacket. The length of this evaporator section was 8 cm.

Several individual determinations were required with each heat pipe to establish maximum heat transfer capability as a function of heat pipe temperature. The general procedure can be described by referring to Fig. 4. This figure shows the maximum and minimum heat removal rates which could be achieved with the test apparatus. Although each curve shows heat removal rates for a single gas, the entire area between the two curves could be covered by using different mixtures of helium and argon in the gas annulus. As previously mentioned, the argon curve was followed until a predetermined heat pipe temperature was reached. Heat removal was then increased by gradually substituting helium for argon in the gas annulus. The test temperature was held essentially constant by increasing the heat input to compensate for the gas change. This heat transfer increase at constant temperature is represented by the vertically arranged points in Fig. 4. Usually, a heat transfer limit was found at some point before a complete gas substitution was made. When a limit was reached, the temperature of the condenser would drop significantly. At visible temperatures, a more positive indication was obtained by watching the evaporator section within the heating coil. When a limit was reached, this section would suddenly increase in temperature until

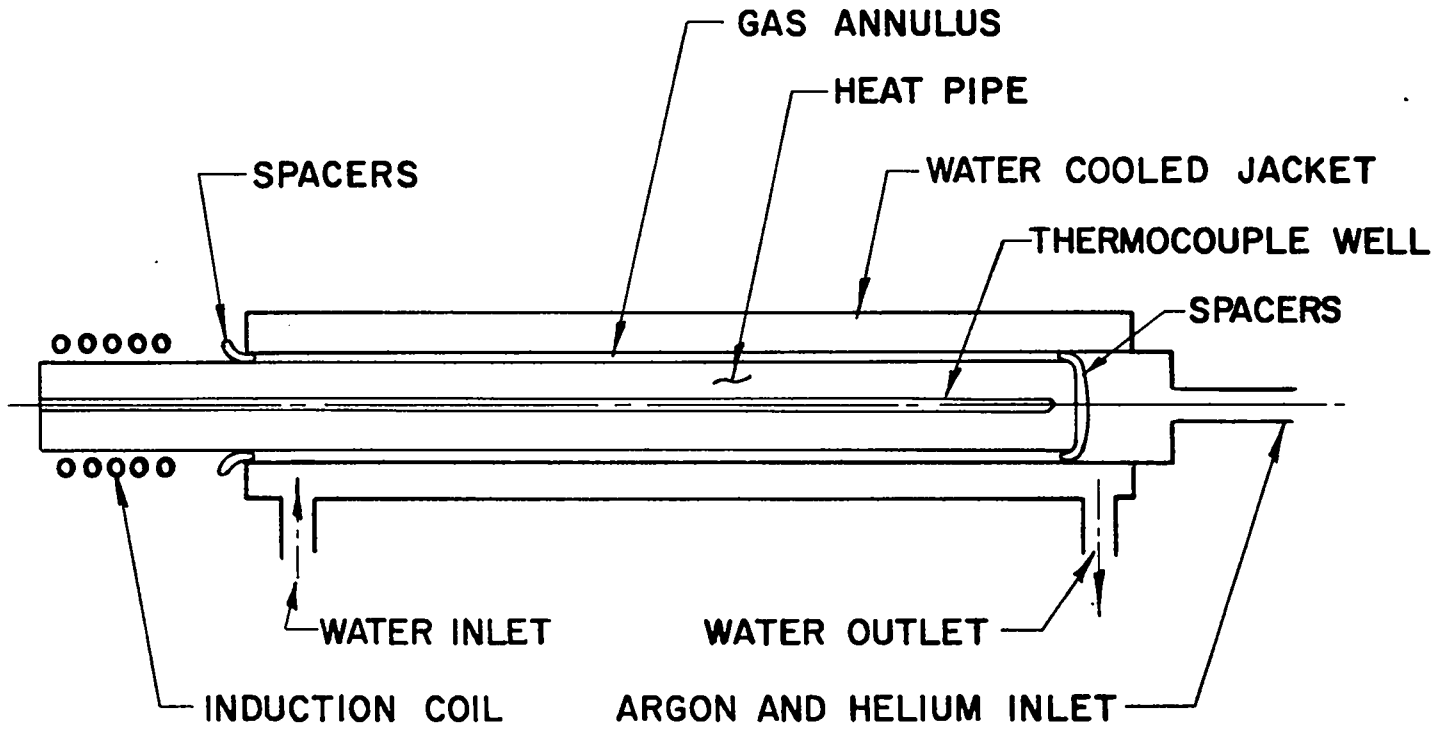

Fig. 3. Heat Transfer Test Apparatus

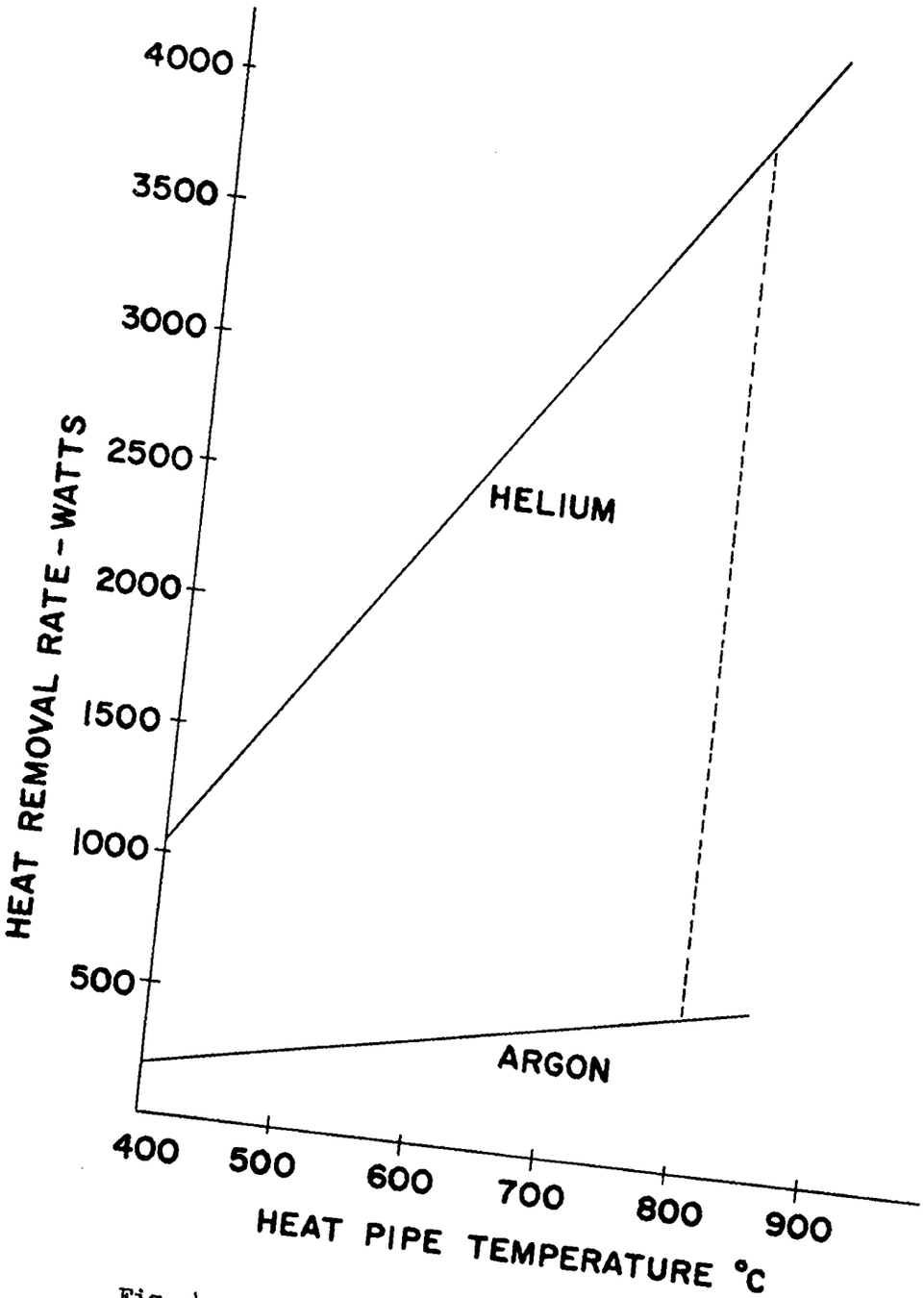

Fig. 4. Heat Removal Range vs Temperature

the input power was shut off. The foregoing procedure was repeated at several test temperatures until a satisfactory heat transfer limit curve was established for a particular heat pipe system.

Heat Pipe Equations

The heat transfer equations used in this investigation were taken from reports by Cotter[1] and Grover, Bohdansky and Busse.[2] The equations were simplified by assuming a negligible gravity effect, uniform heat addition and removal and perfect wetting of the heat pipe structure by the working fluid. The equations, symbols used and some explanatory statements follow:

$$\Delta P_v + \Delta P_\ell = \Delta P_c \tag{1}$$

$$\Delta P_v = \frac{(1 - 4/\pi^2)\, Q^2}{8R^4 \rho L^2} \qquad \text{(For all experiments)} \tag{2}$$

$$\Delta P_\ell = \frac{4\nu ZQ}{\pi N k^4 r^4 L} \qquad \text{(For channels)} \tag{3}$$

$$\Delta P_\ell = \frac{b\nu ZQ}{2\pi(R_w^2 - R^2)\, \epsilon r_c^2 L} \qquad \text{(For screen)} \tag{4}$$

$$\Delta P_c = \frac{\gamma}{r} \qquad \text{(For open channels)} \tag{5}$$

$$\Delta P_c = \frac{2\gamma}{r_c} \qquad \text{(For covered channels)} \tag{6}$$

The symbols used are:

ΔP_v = pressure drop in vapor phase
ΔP_ℓ = pressure drop in liquid phase
ΔP_c = maximum capillary force
Q = maximum heat flow in axial direction
L = latent heat of vaporization
ρ = mass density of vapor
ν = kinematic viscosity of liquid
γ = surface tension of liquid

R = radius of vapor passage

Z = length of heat pipe

r = half-width of channels

N = number of channels

k = channel shape factor

R_w = outside radius of screen structure

r_c = effective radius of screen openings

b = screen permeability factor

ϵ = screen void fraction

1. Equation 1 determines the limiting condition for axial heat transfer. At this point, the drag of vapor and liquid equals the surface tension forces in the capillary structure. Heat transfer limits can be calculated by proper substitution of the remaining equations.

2. Special requirements for the use of Equation 2 are reported by Cotter.[1] In essence, this equation can be used to calculate the vapor pressure drop for laminar flow when inertial forces predominate. This vapor flow regime is characterized by decreasing pressure in the direction of flow within the evaporator and increasing pressure in the direction of flow within the condenser. (Temperature measurements made during the heat pipe experiments confirmed the use of Equation 2.)

3. Equations 3 and 4 can be used to calculate liquid pressure drop when viscous forces predominate. For open channels, the liquid pressure drop is obtained from Equation 3. For screen-covered channels, two parallel paths are available for liquid flow. Equations 3 and 4 must be used to determine the pressure drop for this structure.

4. Since the radius of meniscus curvature along the length of an open channel is infinite, Equation 5 must be used to obtain the maximum capillary force when channels contact the vapor passage. When a layer of square mesh screen separates the channels from the vapor passage, the two principal radii of meniscus curvature are equal and Equation 6 applies. A discussion of capillary force is given in the next section.

5. It should be noted that the foregoing equations do not cover all possible heat pipe systems and operating conditions. As indicated, liquid pressure drop and capillary force equations must be provided to suit specific wick configurations. Also, different vapor pressure drop equations will be required for different vapor flow regimes. Sometimes, the effect of gravity and fluid wetting must be considered. Further modifications will be required if the heat pipe evaporator and condenser are separated by an insulated section. Many heat pipe situations and their appropriate equations are discussed in the first four references listed at the end of this report.

Maximum Capillary Force

When a liquid surface is characterized by two principal radii of meniscus curvature (r_1 and r_2) the pressure difference across the surface (ΔP) is given by the Laplace-Young equation:

$$\Delta P = \gamma\left(\frac{1}{r_1} + \frac{1}{r_2}\right)$$

If working fluid wets a wick perfectly, this equation can be used to determine the maximum capillary force (ΔP_c) in a heat pipe, because when a heat transfer limit is reached, the curvature of the liquid meniscus will be defined exactly by the wick structure.

Maximum capillary force can be explained by referring to the wick structures tested in this investigation. When open channels contact the vapor passage, the radius of meniscus curvature along the length of a channel is infinite and is not effective in determining the capillary force. Only the radius across a channel need be considered. During steady state operation, this radius will be smallest at the evaporator end of a heat pipe and will diminish as heat transfer is increased until it equals the half width of a channel. At this point, a heat transfer limit will be reached and the maximum capillary force will be achieved as shown in Equation 5. When channels are covered with square mesh screen, the two principal radii of the liquid meniscus are equally effective, and

the maximum capillary force is given by Equation 6. If the effective radius of the screen openings equals the half width of the channels, the available capillary force will be doubled by the screen cover.

Pertinent Fluid Properties

Heat pipe capability will vary with temperature as determined by vapor density, liquid kinematic viscosity, liquid surface tension and the latent heat of vaporization of the working fluid. Vapor density is particularly important during heat pipe startup since this fluid property can vary several orders of magnitude before an operating temperature is reached. The values of physical properties used in this investigation are plotted as a function of temperature in Figs. 5 through 8. Vapor densities were calculated from vapor pressure data given in the Handbook of Chemistry and Physics.[5] Kinematic viscosities were calculated from Andrade's equation[6] by using the empirical constants given in the Liquid Metals Handbook.[7] Surface tension values were obtained from published data of J. W. Cooke[8] for potassium and J. W. Taylor[9] for sodium. The variation of latent heat of potassium with temperature was obtained from a report by Walling, Nuzum and Lemmon.[10] The latent heat of sodium was taken as 1000 cal/gm at all temperatures.

Heat Pipe Test Variations

Heat transfer limits were calculated for several 3/4-inch-O.D. x 12-inch-long heat pipes. Temperature, working fluid and wick variations were considered. An estimate was made of the heat removal capability of the experimental apparatus. Ten heat pipe systems were then chosen to provide heat transfer information within the range dictated by the equipment. This range was not sufficient to permit testing of optimum systems, so variations were established to indicate the direction for optimum design. Table I lists the heat pipe variations tested in this investigation.

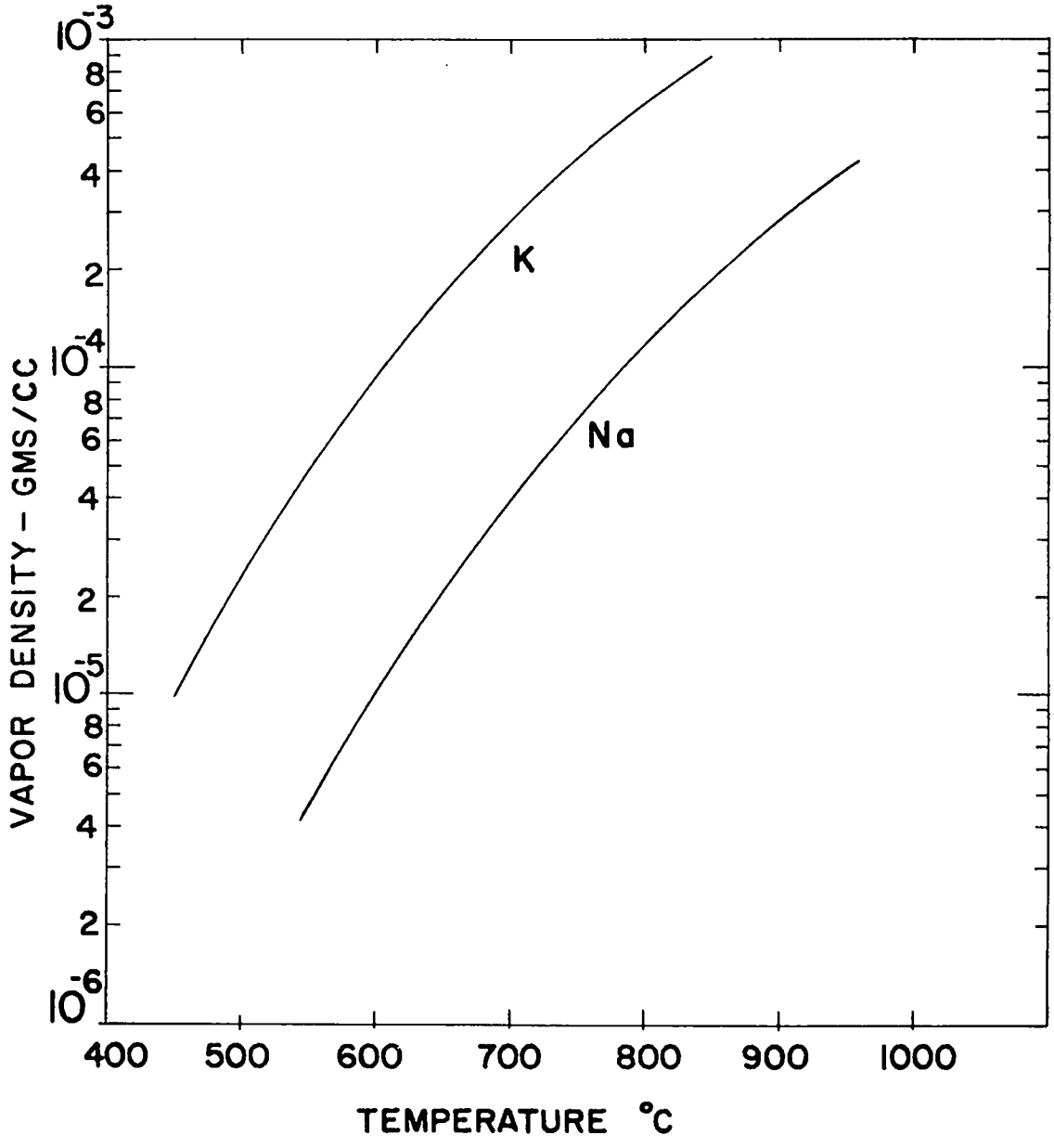

Fig. 5. Vapor Density vs Temperature of Potassium and Sodium

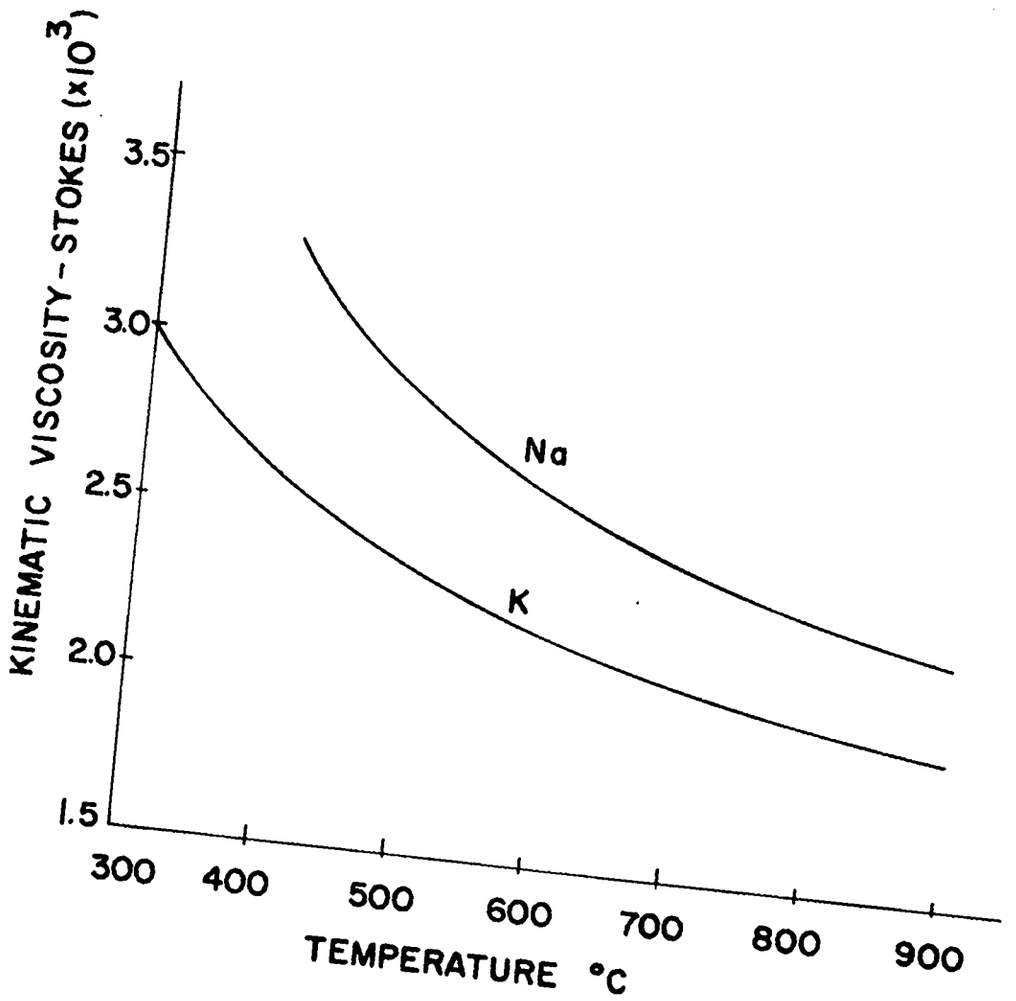

Fig. 6. Kinematic Viscosity vs Temperature of Potassium and Sodium Liquid

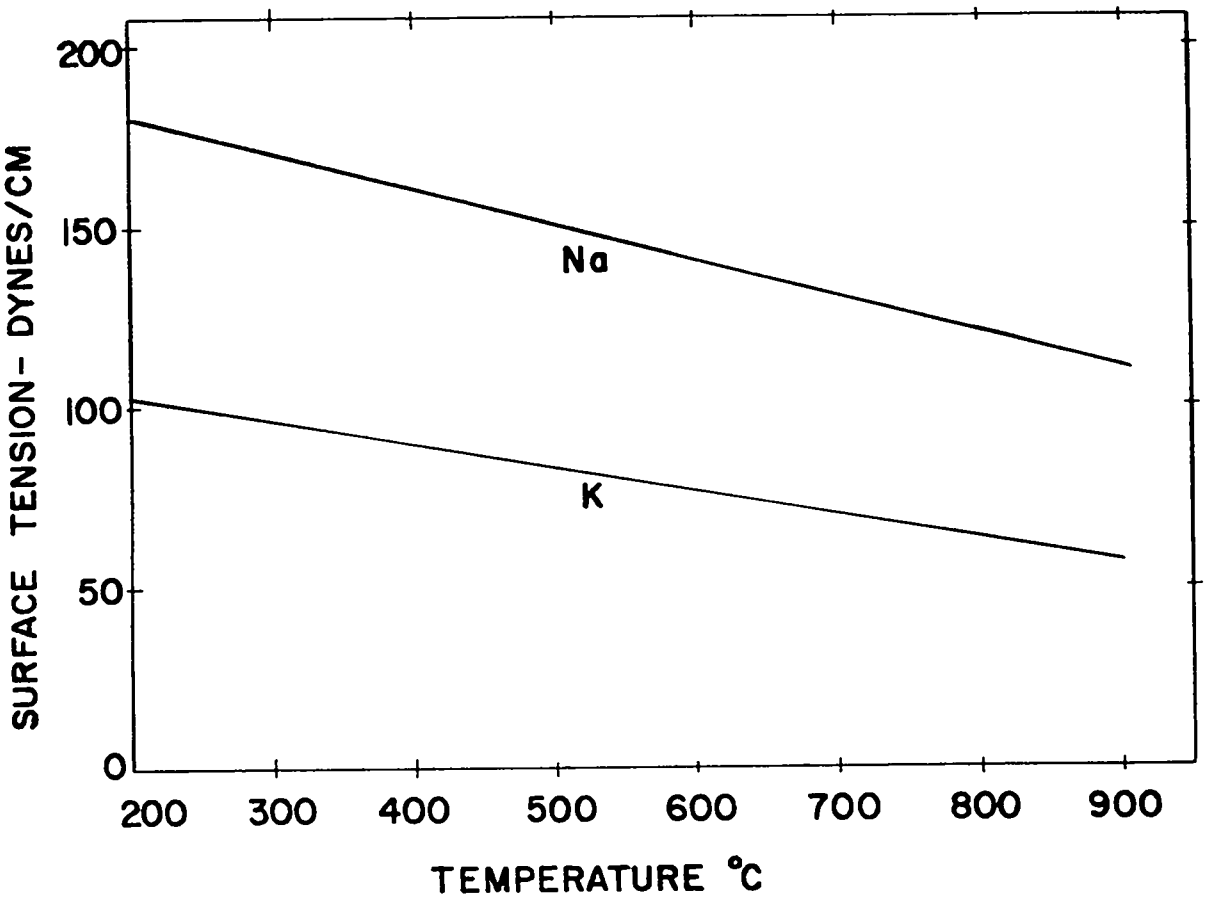

Fig. 7. Surface Tension vs Temperature of Potassium and Sodium

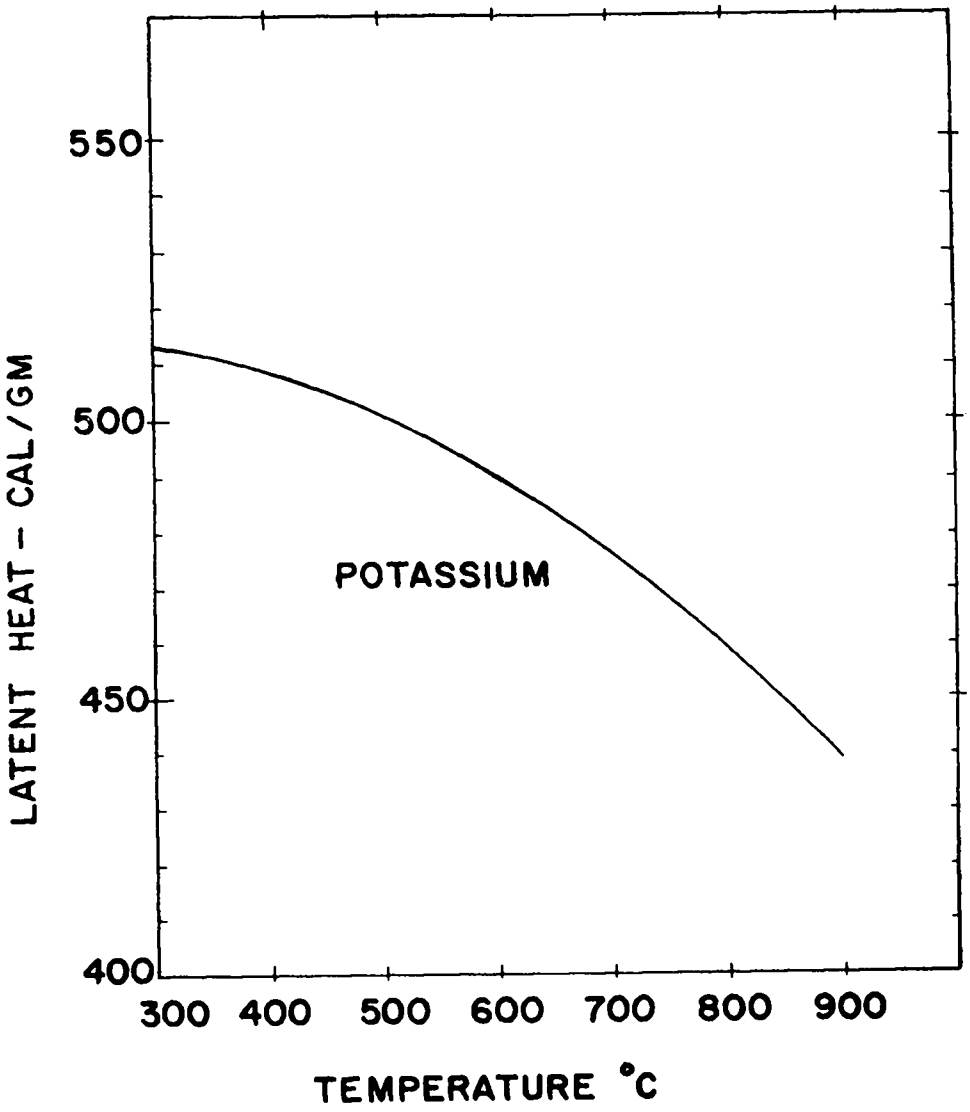

Fig. 8. Heat of Vaporization vs Temperature
(From Walling, Nuzum, and Lemmon)

TABLE I

HEAT PIPE TEST VARIATIONS

Heat Pipe Test No.	Working Fluid	No. of Channels	Channel Size mm		Without Screen	With Screen	
			Width	Depth		Tight	Loose
1	Na	88	0.16	0.40	x		
2	Na	88	0.16	0.40		x	
3	Na	88	0.12	0.30	x		
4	Na	88	0.20	0.50	x		
5	Na	39	0.40	0.50	x		
6	Na	88	0.20	0.50		x	
7	Na	39	0.40	0.50		x	
8	K	88	0.16	0.40		x	
9	K	88	0.16	0.40			x
10	K	88	0.12	0.30			x

Certain geometrical factors, other than those given in Table I, were held constant to simplify the interpretation of experimental results. Some measured values were obtained for the particular factors involved. This information is presented in Table II.

TABLE II

SOME HEAT PIPE TEST CONSTANTS

Geometrical Factors	Values Used
Vapor Passage Radius (R)	0.75 cm
Heat Pipe Length (Z)	30 cm
Evaporator Length (Z_e)	8 cm
Condenser Length (Z_c)	22 cm
Channel Shape Factor (k)	1.5 (1.2 for Tests 5 and 7)
Effective Screen Radius (r_c)	0.08 mm
Screen Thickness (R_w - R)	0.22 mm
Screen Permeability Factor (b)	12
Screen Void Fraction (ϵ)	0.5

Channel shape factors were estimated for open and screen covered channels by using the hydraulic radius method:

$$k = \frac{2}{r}\left(\frac{\text{flow area}}{\text{wetted perimeter}}\right)$$

Here, as in Equation 3, r equals the half width of the channels. For open channels, an allowance was made for the reduced flow area caused by the liquid meniscus. For screen covered channels, the complete flow area was used, but the wetted perimeter was increased only by the amount actually covered by the screen material. The screen covering was such that almost identical shape factors were obtained for open and screen covered channels having the same depth to width ratio. To check this method of calculation, values were estimated and then determined experimentally for channels completely covered by a solid material. The experiments were done by expanding a rubber tube against the inside wall of various heat pipes and measuring water flow through the channels as a function of head. Excellent agreement between experimental and calculated values was obtained and, as expected, the channel shape factor was somewhat smaller for completely covered channels.

A convenient method for calculating screen permeability and screen void fraction was not available. Values for these factors were obtained from some earlier heat pipe experiments where this type of screen was used.

Heat Transfer Results

The experimental results obtained in this investigation are plotted as a function of heat pipe temperature in Figs. 9 through 12. The figures are arranged to show how maximum heat transfer is affected by a particular heat pipe variation. Each data point represents an individually determined heat transfer limit as described in the experimental procedure. Solid lines represent limiting curves which were established for different test heat pipes. Some calculated curves are also presented so that experimental results can be compared with predicted values.

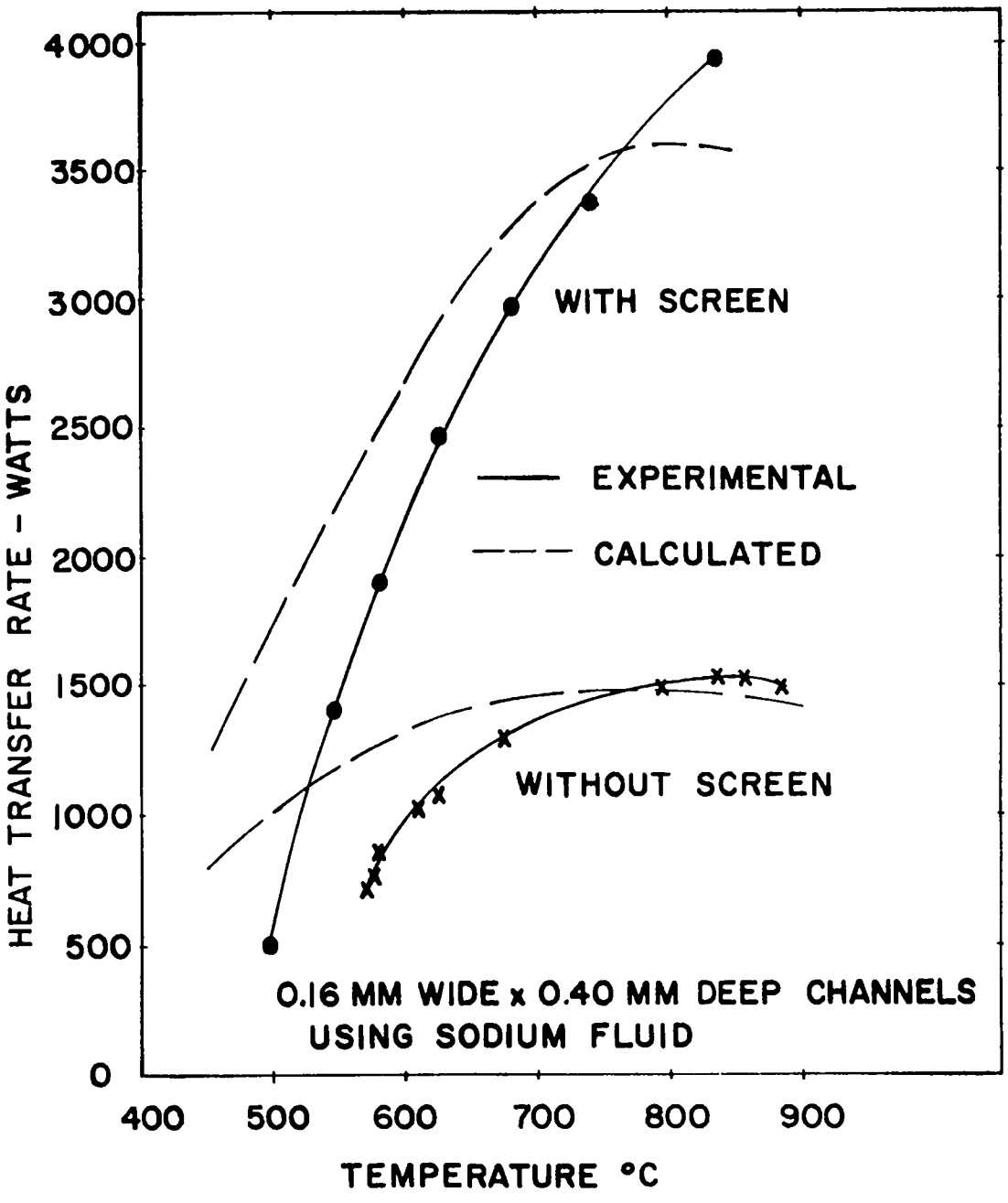

Fig. 9. The Effect of Screen on Axial Heat Flow with Channels

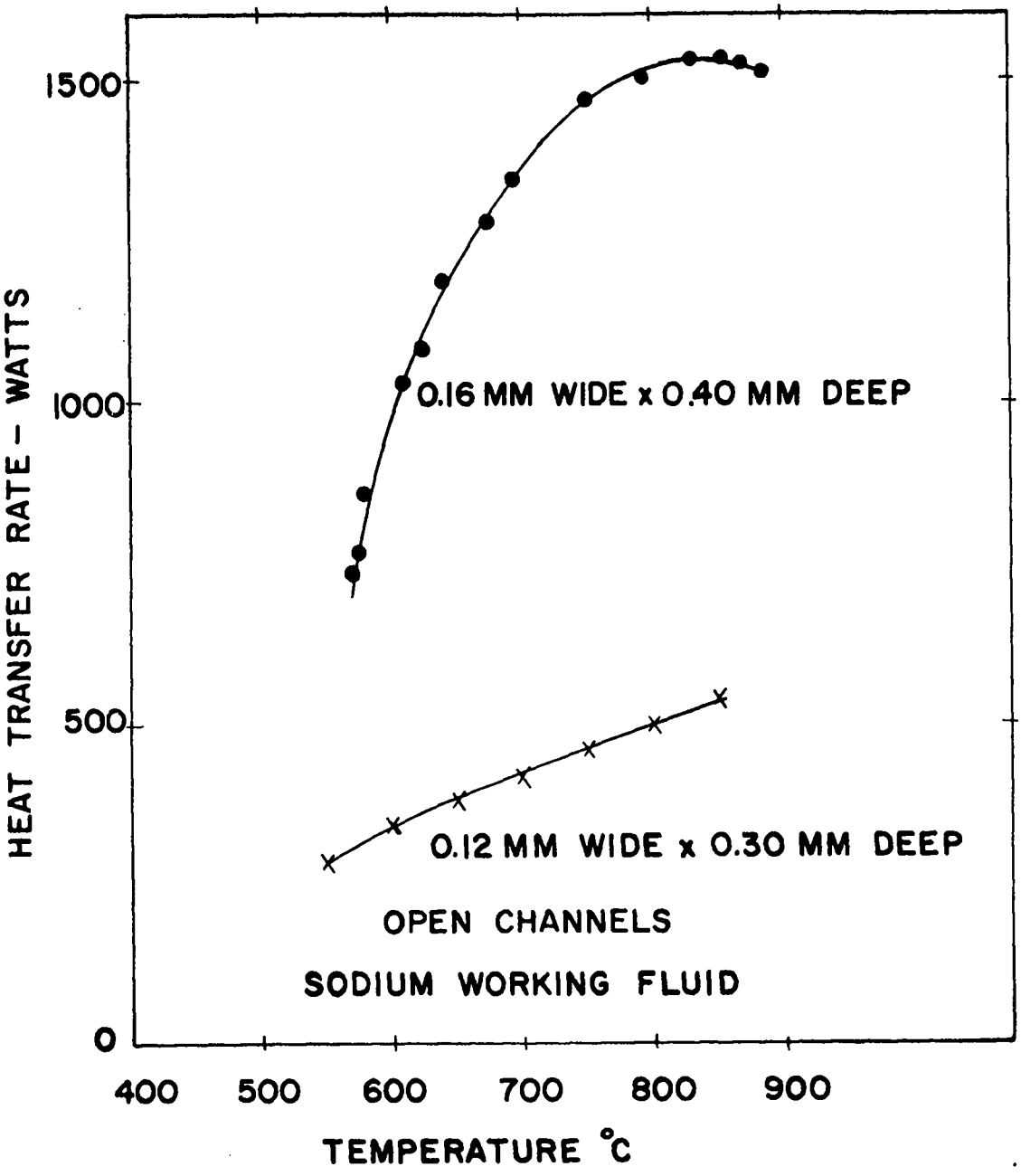

Fig. 10. The Effect of Channel Size on Axial Heat Flow

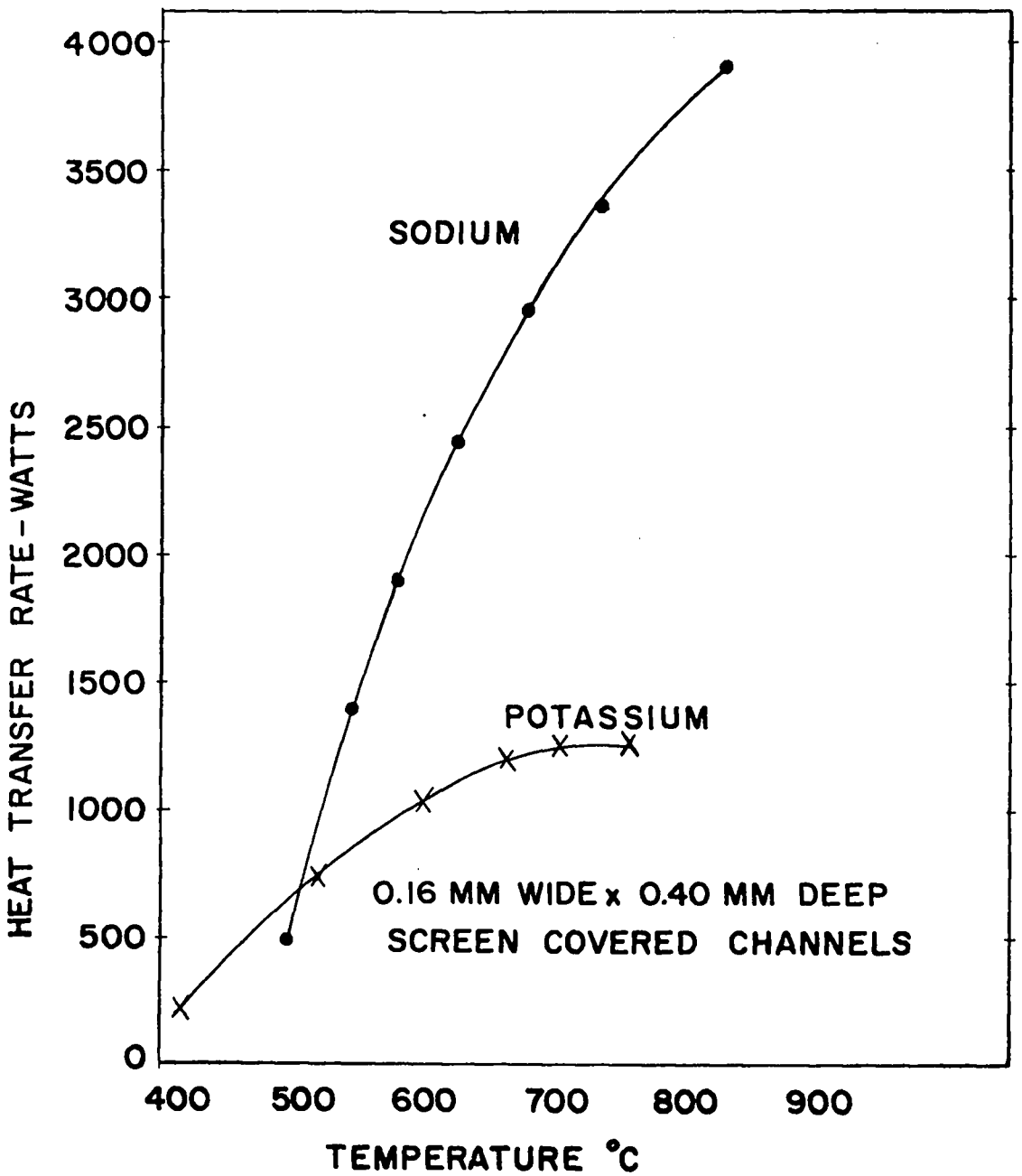

Fig. 11. The Effect of Fluid on Axial Heat Flow

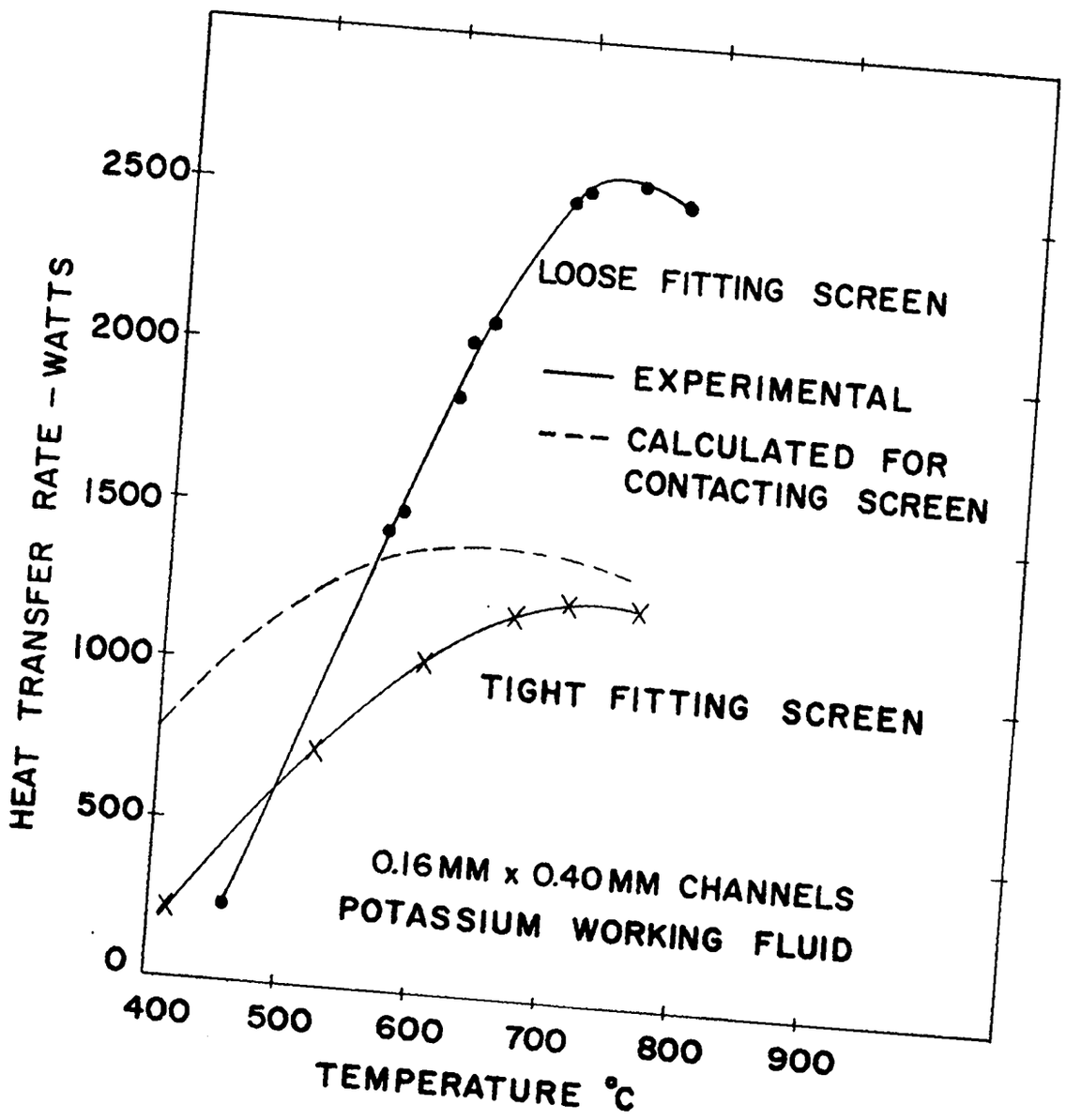

Fig. 12. The Effect of Screen Fit on Axial Heat Flow with Channels

The results obtained during Tests 1 and 2 are compared in Fig. 9. This figure shows the effect of a screen liner with sodium as the working fluid. Measured heat transfer limits are compared with calculated limits.

The results of Tests 1 and 3 are compared in Fig. 10. This figure shows how increased channel size permits greater heat transfer with open channels. However, the curves indicate that this may not be the case during startup and at low operating temperatures. This indication was verified during Tests 4 and 5 with larger open channels. These heat pipes could not be started in the heat removal system.

The results of Tests 6 and 7 are not plotted because heat transfer limits were found only at low operating temperatures. At temperatures above 600°C, the heat transfer capability of the heat pipes exceeded that of the heat removal apparatus. These tests emphasize the advantage of a screen covering since the same heat pipes could not be started with open channels.

The effect of different working fluids is shown in Fig. 11. Results of Tests 2 and 8 are compared.

Since potassium has relatively poor properties for heat pipe operation, it can be used to advantage for wick improvement studies. A simple test along these lines was accomplished by replacing the screen used in Test 8 with a loose fitting screen for Test 9. The results of these two tests are compared in Fig. 12. A curve is also presented to show calculated heat transfer values for screen contacting the wall and channels. The increased heat transfer, obtained with the loose fitting screen, is probably due to an additional flow path between the screen and the wall which reduces the pressure drop of the returning liquid.

The results of Test 10 confirm the effect of loose fitting screen. Although smaller channels were used in this test, heat transfer limits at most temperatures were reasonably close to those obtained for Test 9. These heat transfer limits are compared in Table III.

TABLE III

COMPARISON OF TESTS 9 AND 10

	Heat Transfer Limit, Watts	
Temperature, °C	Test 9	Test 10
450	200	620
500	740	1120
550	1280	1570
600	1800	1890
650	2230	2130
700	2530	2310
750	2560	2380

An additional experiment was performed in order to demonstrate the excellent heat transfer properties of lithium. Test 3 was repeated with a niobium-1 w/o zirconium alloy container and lithium working fluid. (This particular test geometry was chosen because it showed the poorest heat transfer characteristics with sodium and, therefore, would allow measurements at modest power levels with lithium.) Since the vapor pressure (vapor density) of lithium is much lower than sodium, the system was difficult to start and would not operate properly at temperatures below 800°C. At 850°C, however, heat transfer was limited at 2000 watts with lithium, compared to 550 watts with sodium. At 1150°C, heat transfer was limited at 4000 watts. Above 1150°C, limits could not be established since they exceeded the capability of the heat removal equipment.

Discussion of Results

Since this investigation was designed to show significant heat transfer variations, the actual magnitude of the differences obtained was not surprising. However, the relatively good agreement between calculations and experiments at higher temperatures was not expected because of the use of approximate dimensional factors and fluid properties. The greater difference between theory and experiment at lower temperatures

must be explained by a momentum interaction between low density, high velocity vapor and returning liquid. This effect is particularly detrimental with open channels, as evidenced by Tests 4 and 5 where startup was impossible.

The use of screen may reduce the amount of interaction between vapor and liquid, but the reduction may not be complete. A more apparent screen advantage results from the increased capillary driving force when open channels are covered with screen. (This effect is predicted by heat pipe equations and has already been discussed in that section.) It may be possible to achieve very high heat transfer rates by using relatively fine screen over coarse channels provided the tensile strength of the liquid is not exceeded in this manner.

The effect of increased channel size could not be tested extensively in this investigation. Certainly, optimum heat pipe systems for space applications may require significantly larger capillary passages than those tested. The results of this investigation indicate that such systems may be feasible, provided heat transfer rates can be limited during startup and a screen is used to cover these larger channels.

Heat transfer differences were expected for potassium and sodium, based on fluid property information. Although sodium should be a better working fluid for most applications, potassium may be advantageous whenever vapor pressure drop tends to control heat transfer (low temperature, small vapor passage).

The use of loose fitting screen apparently provides a means for lowering the liquid pressure drop while maintaining a high capillary driving force. Substantially greater heat transfer rates may be realized with this type of structure by optimizing the size of the annular passage for liquid return.

Although the heat transfer capability of lithium could not be fully demonstrated in this investigation, the advantage of this fluid is indicated in the last experiment. This experiment also shows how fluid vapor density controls the temperature behavior of heat pipes. Because of its

vapor pressure, lithium can be operated at much higher temperatures than potassium and sodium without exceeding the strength of its container. However, because of its relatively low vapor density, heat pipe startup may sometimes be difficult with this fluid, and operating temperatures well above 800°C may be required before it can be used to real advantage.

Heat Pipe Startup Behavior

Heat pipe startup behavior is difficult to predict and may vary considerably, depending on many factors. The effects of working fluid and wick configuration were studied in this investigation. Quantitative information was not obtained, but a general description of startup behavior can be presented at this time.

During startup, vapor must flow at relatively high velocity to transfer heat from the evaporator to the condenser of a heat pipe, and the pressure drop through the vapor passage will be large. Since the axial temperature gradient in a heat pipe is determined by the vapor pressure drop, the temperature of the evaporator will be much higher than the condenser when heat is first added. The evaporator section will quickly reach some temperature level, depending on the working fluid. If the heat input is large enough, this temperature will move into the condenser section with a rather distinct front. During normal heat pipe startup, the temperature of the evaporator will increase a few degrees until the front reaches the end of the condenser. At this point, the temperature of the condenser will increase, and the heat pipe structure will become nearly isothermal. (When lithium or silver are used as working fluids, this entire operation occurs at visible temperatures and has been observed many times.)

Heat pipes with screen covered channels behaved normally during startup as long as heat was not added at too fast a rate. When potassium was used as a working fluid, the temperature of the evaporator leveled out at about 400°C when heat was first added. In Test 8, where tight fitting screen was used, the heat pipe structure became nearly isothermal

at 420°C. In Tests 9 and 10, where loose fitting screen was used, this condition was reached at 450°C. In Tests 2, 6 and 7, tight fitting screen and sodium were used. In these tests, the evaporator first leveled out at about 490°C and the heat pipes became nearly isothermal at 500°C. This higher startup temperature was expected with sodium because of its vapor density (see Fig. 5).

Heat pipes with open channels did not behave in the manner just described. Tests 4 and 5 could not be started in the heat removal apparatus and, as previously mentioned, heat transfer information was not obtained for these systems. Although Test 1 could be conducted as indicated in the experimental procedure, very large temperature gradients developed during startup and isothermal conditions were obtained in a peculiar manner. When heat was first added, the temperature of the evaporator leveled out at about 525°C and the normal 490°C front extended only a short distance into the condenser. In order to achieve a nearly isothermal condition, more heat was added, but the temperature of the evaporator did not increase uniformly. A temperature of 800°C was measured optically between the two induction coil turns farthest from the condenser. Most of the evaporator remained at 525°C, and a sharp gradient existed between the two temperature regions. Enough heat was added so that, eventually, the 490°C front reached the end of the condenser; but before this happened, temperatures in excess of 800°C were observed between the first four induction coil turns. Fortunately, once the condenser became nearly isothermal, its temperature increased and the very hot evaporator region rapidly cooled in a pattern which suggested the return of liquid through channels. From this point on, the heat pipe behaved quite normally.

The heat pipes used in Tests 3, 4 and 5 could not be started when the standard 22-cm condenser length was located in the calorimeter system. In each of these tests, the condenser never became isothermal although the entire evaporator was heated above 800°C in an attempt to achieve this condition. Heat transfer limits were obtained in Test 3 because

this heat pipe could be started when an 18-cm condenser length was used. As shown in Fig. 10, these heat transfer limits were well below those encountered in Test 1, and this may explain the greater startup difficulty. Although smaller channels were used in Test 3 and lower heat transfer limits were predicted, a startup problem was not expected in either system. In any event, this problem cannot be explained exclusively in terms of heat pipe capability. Higher heat transfer limits were predicted for the larger channel systems used in Tests 4 and 5, and these heat pipes were impossible to start.

Startup difficulties and the low heat transfer limits encountered at low temperatures appear due to an interaction between the vapor flowing in the central passage and the liquid returning through the wick. During startup, the vapor density is low and its velocity can be high enough to prevent the liquid from returning to part of the evaporator. Although the amount of interaction is not easy to estimate, its general dependence on vapor temperature, vapor passage diameter, heat pipe length and wick configuration is fairly obvious. Screen covered channels may be suitable for many applications, but different wick structures may provide a more effective baffle between vapor and liquid. Longer heat pipes are currently being tested to find better wick systems and to provide a more complete understanding of startup behavior.

Conclusions

The heat transfer characteristics of heat pipes with fixed outside dimensions can be changed significantly by variations in wick structure. The practical operating temperature range for such systems will be determined by the vapor density of the working fluid. Within this temperature range, heat transfer limits can be predicted with some confidence by using existing heat pipe equations. At lower temperatures, a momentum interaction between vapor and returning liquid can seriously limit heat transfer and may prevent heat pipe startup. Heat transfer capability and heat pipe startup behavior can be substantially improved by the use of a two component wick structure.

References

1. T. P. Cotter, "Theory of Heat Pipes," LA-3246-MS, February, 1965.
2. G. M. Grover, J. Bohdansky and C. A. Busse, "The Use of a New Heat Removal System in Space Thermionic Power Supplies," EUR 2229.e (EURATOM) 1965.
3. J. Bohdansky and H. E. J. Schins, "Heat Transfer in Heat Pipe Operating at Emitter Temperatures," International Conference on Thermionic Electrical Power Generation, London, 20-24 September, 1965.
4. W. A. Ranken and J. E. Kemme, "Survey of Los Alamos and Euratom Heat Pipe Investigations," Thermionic Conversion Specialist Conference, San Diego, 25-27 October, 1965.
5. Handbook of Chemistry and Physics, 44th Edition, 1962-1963.
6. E. N. da C. Andrade, Phil. Mag. 17, 698 (1934).
7. Liquid Metals Handbook, 3rd Edition, Sodium (NaK) Supplement, June 1955.
8. J. W. Cooke, ORNL-3571, 85-88, December 31, 1963.
9. J. W. Taylor, "Wetting by Liquid Metals," Progress in Nuclear Energy, Series V, Vol. 2, 398-416 (1959).
10. J. F. Walling, H. K. Nuzum and A. W. Lemmon, Jr., "The Vapor Pressure and Heat of Vaporization of Potassium from 480 to 1150°C," BATT-4673-T3, April 30, 1963.


RECEIVED
OCT 31 1966
Los Alamos
Scientific Laboratory
P. O. Box 1663
Mail & Records

[redacted]